

Developing insights using CFD – Tail rotor CFD analysis and design

Alan Brocklehurst¹, Rene Steijl and George Barakos

Department of Engineering, University of Liverpool,
Brownlow Hill, Liverpool L69 3GH, United Kingdom

e-mail: g.barakos@liverpool.ac.uk

¹PhD student and Principal Engineer, Rotor Aerodynamics, AgustaWestland (Yeovil).

Key words: Tail rotor design, tip shape, hover induced power, CFD.

Abstract: A CFD method has been employed for the computation of the flow around hovering tail rotors of various tip designs. All rotors start from the same simple configuration and employ square, swept-leading-edge, or Kuchemann tips, some of which are equipped with anhedral. Variations of blade twist were also considered. The method was first validated against available published experimental data and is further compared to tests on a model tail rotor in hover, and subsequently used for the analysis of all tail rotor designs put forward. The results of the computations indicate that, at low thrust, the Euler equations are adequate for representing the differences between the various tip shapes, at least as far as the induced power is concerned, while Navier-Stokes equations are needed as the pitch setting and thrust becomes higher. The current Helicopter Multi-Block (HMB) CFD method has adequate resolution to highlight differences in tip shape and consequently may be used for the preliminary design and analysis of helicopter blades. The effects of twist and anhedral were also well-represented, and it was found that anhedral off-loads the tip, increasing the loading at mid-radius, in a broadly similar manner to twist.

1. INTRODUCTION

The design and analysis of helicopter rotors has traditionally been based on extensive wind tunnel and flight experimentation, complemented by numerical analyses using either combinations of strip theory and lifting-line/surface approaches with prescribed/free-wake modelling [1]. Such techniques have been fairly successful in providing the basic information needed for the evaluation of rotors and for many years have represented the established methodology used by helicopter manufacturers. One of the problems with this low-order-approximation approach is associated with uncertainties in modelling the flow-field near the tip of the rotor blades. The flow in the tip region is dominated by three-dimensional effects, including vortex formation, viscous separation and compressibility, all of which are influenced by the tip planform shape and changes in incidence, side-slip (in forward flight) and Mach number.

CFD is ideally suited to simulating the complex 3D aerodynamics of the rotor, since the method makes use of the fundamental conservation laws for mass, momentum and energy, together with the precise surface geometry and given flow-field boundary conditions. This modern approach - after proper validation - appears ideal for the study of rotor tip flows since three-dimensionality, viscous effects and compressibility are represented by the general framework of the Navier-Stokes equations without any additional modelling or corrections.

In this paper, a comparison of several tail rotor designs is presented in an effort to develop understanding of the influence of tip shape on rotor performance and to quantify the effects of the various design features such as blended Kuchemann tip shapes, anhedral and twist. All results presented in this paper have been obtained using the Helicopter Multi-Block solver (HMB) [2,3].

The paper begins with a brief presentation of the solver and proceeds to its validation using available experimental data. This step is followed by a presentation of the various designs considered during this study along with the obtained results at a range of thrust settings. The effects of twist and anhedral are then considered, before comparing the relative predictions of inviscid and viscous cases. A summary of the findings along with suggestions for further work are given at the end of the paper.

2. THE HELICOPTER MULTI-BLOCK SOLVER

The Helicopter Multi-Block (HMB) solver has been under development at Liverpool University for the past three years and has been validated and demonstrated for a range of test cases related to helicopter flow analysis and design.

The unsteady Navier-Stokes equations are discretised on a curvilinear multi-block body conforming mesh using a cell-centred finite volume method. The convective terms are discretised using Osher's upwind scheme [4]. MUSCL variable extrapolation is used to provide second-order accuracy with the Van Albada limiter. A central discretisation method is used for the viscous terms. The solver includes a range of one- and two-equation turbulence models and a Smagorinsky LES and Spalart-Almaras DES model. A dual-time stepping method is employed for time-accurate simulations, where the time derivative is approximated by a second-order backward difference [5]. The resulting nonlinear system of equations is solved by integration in pseudo-time using a first-order backward difference. In each pseudo-time step, a linearisation is used to obtain a system of equations, which is solved using a Generalised Conjugate Gradient method with a Block Incomplete Lower-Upper (BILU) pre-conditioner.

The HMB solver makes use of a special scheme for the actuation of rotor blades [3] and has a "hover formulation" which allows the computation of hovering rotor flows as steady-state cases resulting in higher throughput where several rotors have to be tested at a range of thrust settings. In addition, a rotor trimmer is also implemented in HMB and can be used for the analysis of rotors at a specific thrust, either in hover or forward-flight.

To obtain an efficient parallel method based on domain decomposition, the method should have a good serial performance when applied to the domains allocated to the different processes, combined with a minimal communication. To achieve this aim, the flow solver uses the following methods:

The flux Jacobians resulting from the linearisation in pseudo-time are employed in an approximate form that reduces the number of non-zero entries and as a result the size of the linear system. The use of the approximate Jacobian also reduces the parallel communication since only one row of halo cells is needed by the neighbouring process in the linear solver instead of two in the case of an 'exact' Jacobian.

- a. The communication between processes is minimised by decoupling the BILU factorization between blocks.
- b. On each processor a vector is allocated that contains all the halo cells for all grid blocks.
- c. Inter-process communication is performed by sending a series of messages between the respective processes, each corresponding to a block connection, containing the halo cell data. The messages are sent in chunks of 10,000 double precision numbers using non-blocking send and receive MPI function.

This method has been used on a range of platforms, including Beowulf clusters consisting of various generations of Pentium processors and multi-processor workstations. Recently, the solver was ported to the HPCx computer (50 IBM Power4+ Regatta nodes, i.e. 1600 processors, delivering a peak performance of 10.8 TeraFlops) at Daresbury Laboratory.

3. TAIL ROTOR DESIGNS AND CFD GRID GENERATION

Accurate representation of the blade geometry is paramount and this can be achieved with genuinely multi-block grids. Figure 1 summarises the current technique which is based on the idea of surrounding the blades in “rigid” blocks (Fig 1a) of high-quality grids and account for changes of pitch and rotation by deforming the surrounding domain. The grids developed for this work were generated using ICEM-CFD Hexa and then converted in a format suitable for the HMB solver. The number of blocks is mainly dictated by the number of available processors for parallel execution. A typical calculation involves about 250 blocks per blade and is computed on 16-128 processors according to the grid density and solver options employed. A typical computational domain is shown in Figure 1b.

The current topologies combine an H-type structure away from the blades with a C-type structure attached to them. This allows for accurate computation of viscous cases and provides a mechanism for pitching the blades with the near-grid staying in an un-deformed state. Where grid deformation is needed this is done via trans-finite interpolation (TFI). Figure 1c provides the details of the surface topology and also presents the complex multi-block topology near the blade for a case where a hub is also present (Figure 1a).

Figure 2 illustrates the various tip shapes which were created by modification of the rectangular baseline rotor blade. The baseline blade was chosen to be consistent with the zero-twist model rotor blade that was used in the hover tests carried out at Westland Helicopters in the 1980's to investigate the effect of linear twist for the tail rotor. These experimental results are re-employed here to provide a basis for comparison with the CFD.

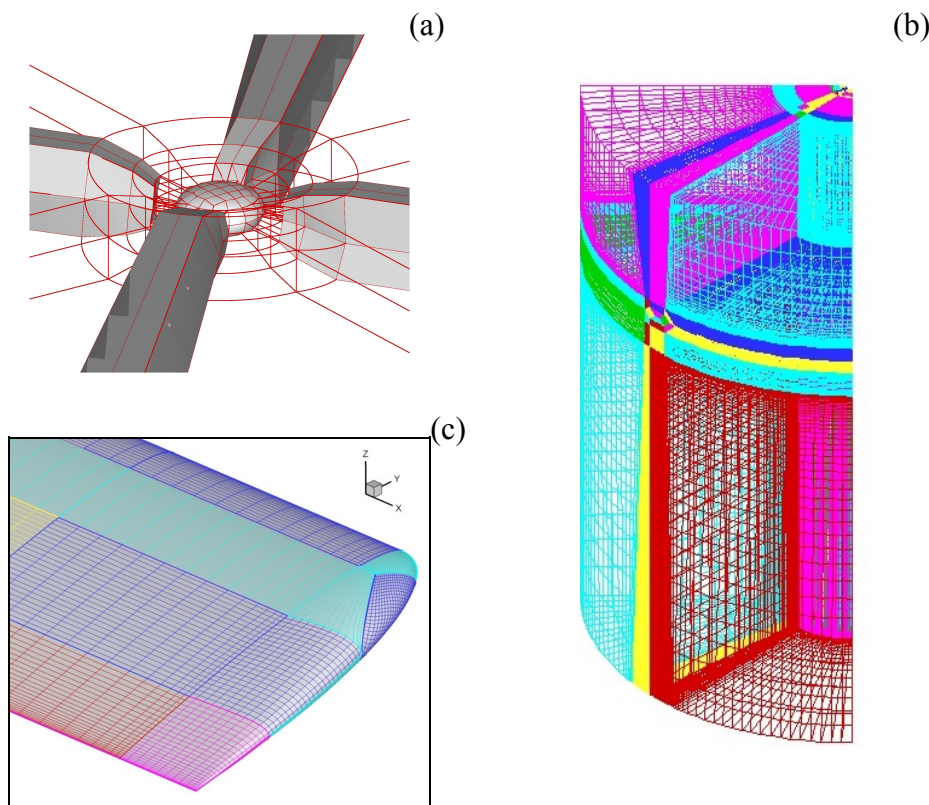


Figure 1. Multi-block grids employed with HMB for the analysis of tail rotor designs. (a) blade-attached blocks, (b) far-field domain and (c) surface topology. The surface topology in (c) is compatible with TRBs 001, 002, 003 and 005. A simpler topology can be used for TRBs 000, 004.

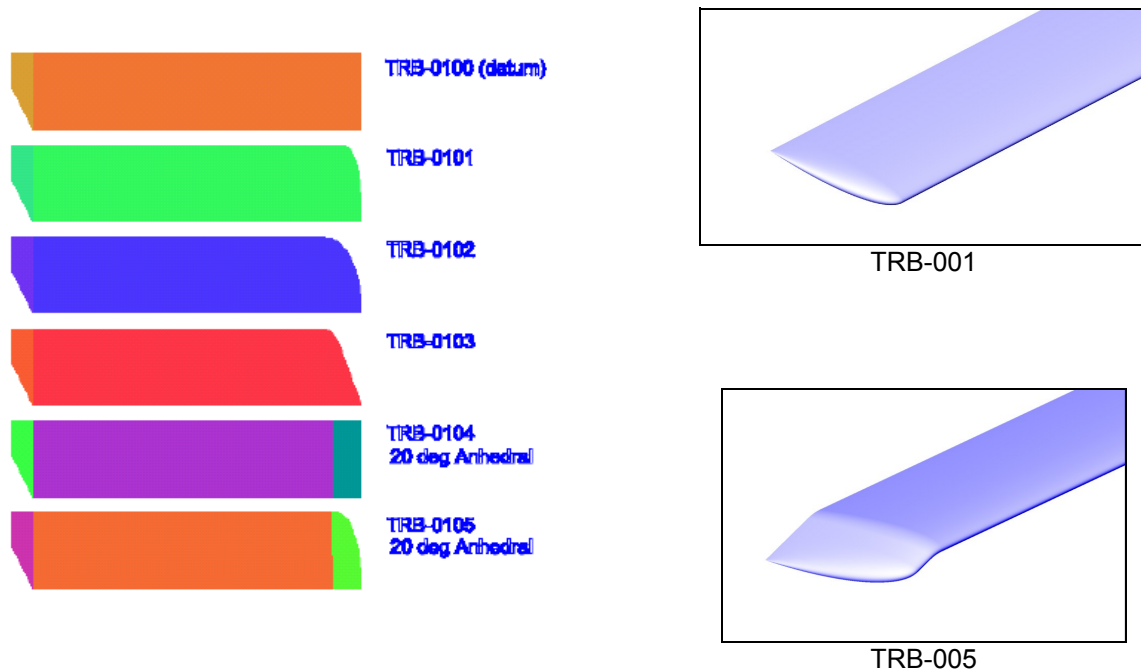


Figure 2. Planform view of the tail-rotor designs considered in this work. Variants of each rotor with added linear twist were also produced.

All blades were defined from a NACA0012 section and have a ratio of $R/c=6.402$ (blade radius to root chord). The same root has been used for all blades and differences are concentrated in the tip region. TRB-000 is the square datum blade while TRB-001 is a version with a $1/4c$ wide Kuchemann tip. TRB-002 again has a Kuchemann-style tip, but with the span-wise extent increased to $1/2c$. TRB-003 employs a 70deg swept back tip design. The remaining two configurations, TRB-004 and TRB-005, are variants of the datum and TRB-001 configurations with anhedral. All rotors considered are 4-bladed and a zero coning angle was specified in the blade tip design studies where a typical full-scale tip Mach number of 0.6 was used. Finally each of the blades can be combined with any value of twist, and surface definitions were prepared to match the model rotor blades which had linear twist of 0, 8 and 16 degrees.

4. VALIDATION OF THE CFD SOLVER IN HOVER

Validation results for hovering rotors, and rotorcraft flows in general, computed with HMB have been previously presented [2-3,6-7]. Further comparisons with test data are presented here. This set of results corresponds to previously unpublished model rotor tests conducted by the first author at Westland Helicopters in 1980/4. For the datum rectangular blade, thrust, power, pitch and vortex wake measurements are available from tests on a 4-bladed model rotor with 0, 8 and 16 degrees of twist, and this data is used to confirm the trends of the Euler CFD predictions before going on to explore the new tip shapes. Excellent agreement was obtained and this established confidence in the CFD method and the grids. The model rotor had stiff composite blades of NACA0012 aerofoil section, with the first aerofoil located at $1/3$ radius. The radius of the blade was 21" (533.4mm) by 3.28" (83.3mm) chord, giving $R/c=6.402$. In the tests, the tip Mach number ranged from 0.263 for the flow visualisation up to a maximum of 0.492 for the force measurements.

Figure 3 compares predicted and measured vortex displacements for the base-line configuration showing excellent agreement between HMB predictions and measurements. The CFD also reveals some small non-linear variations in the vortex displacements, and more particularly in the wake contraction which appear to be reflected in the experimental results. The tests were conducted in a large hover test facility with reduced tip speed to avoid any danger of re-circulation, and the blades were accurately balanced and tracked to avoid vortex gearing.

A separate set of computations on grids of various sizes was also performed in order to establish grid-independent solutions in terms of the resulting figure of merit (FoM) of the rotor. Results from this effort can be seen in Figure 4 where little dependence of the FoM can be seen on grids with more than 2 million cells per rotor blade. As a result of this investigation all generated grids were of the order of 2 million cells per blade and this was kept consistent for the various planform designs.

As also shown later, the Euler results for Figure of Merit in Figure 7 are, of course, higher than they would be in reality, due lack of viscosity, and to overcome this for initial design comparisons a constant skin friction or profile drag coefficient was added to the raw computational results. Taking this into account naturally reduces the sensitivity of the results for the very low pitch case for realistic FoM values, as shown by the thinner lines in Figure 7.

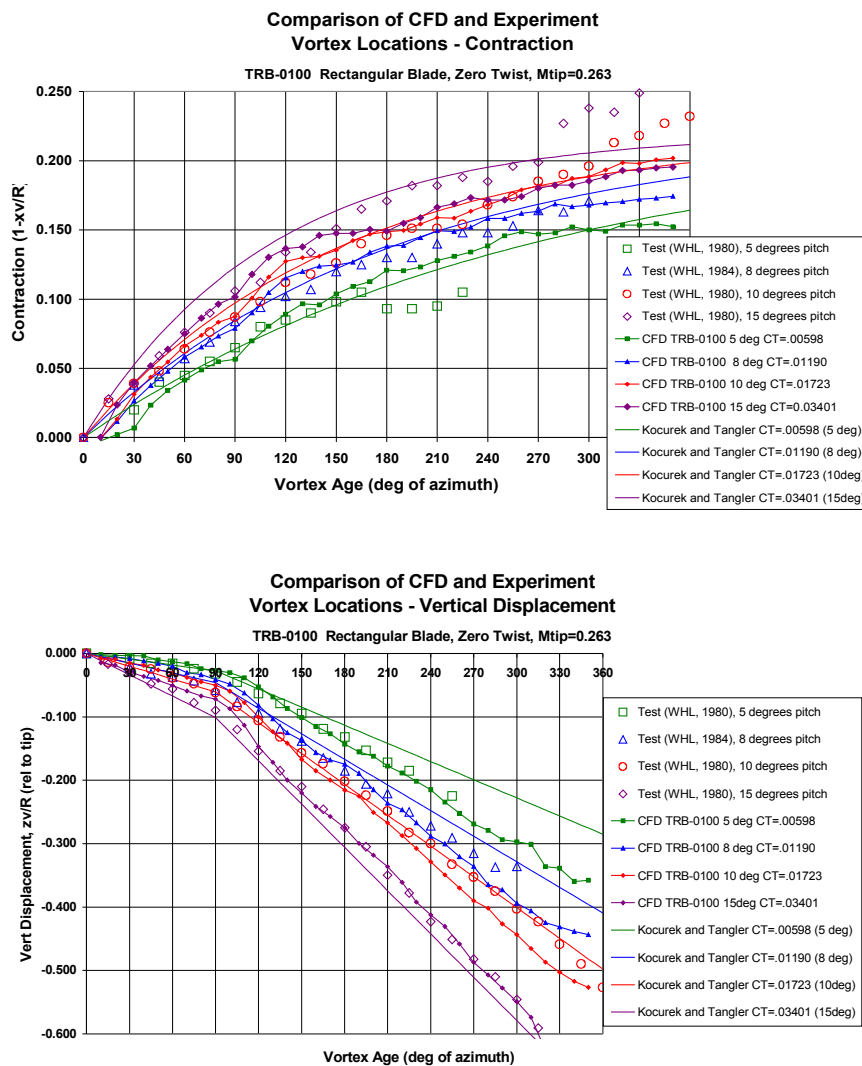


Figure 3. Comparison between experiments and CFD predictions for the location of the tip vortex for the baseline blade. The solid lines represent predictions made with a Kocurek and Tangler wake model [9].

TRB_000_00 Grid Sensitivity Study

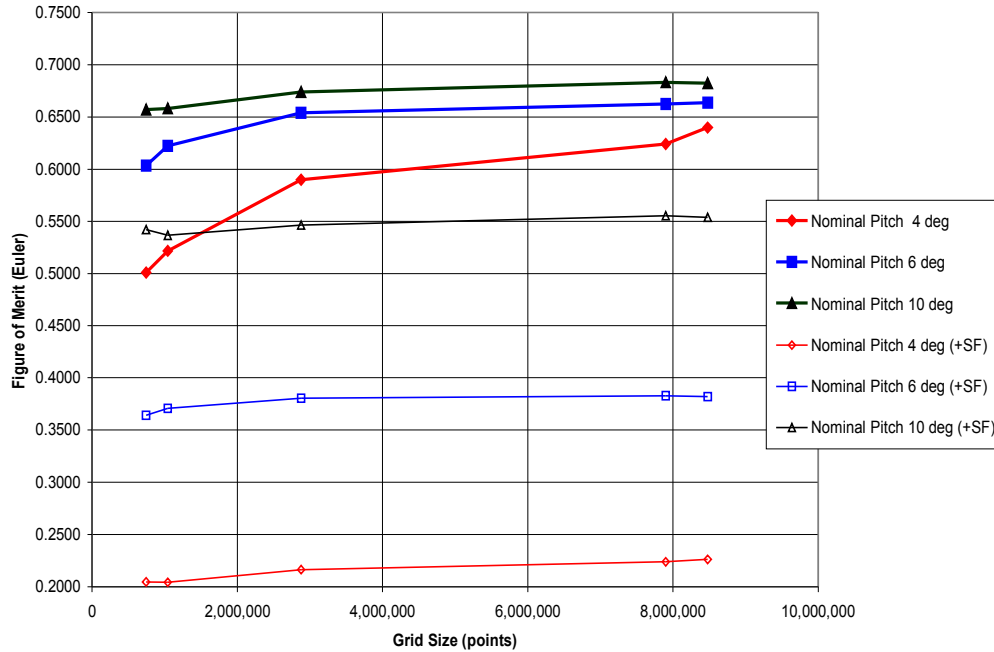


Figure 4. Grid convergence of the CFD solution. The FoM was used as the convergence criterion with grids reaching 8.5 million cells in size.

Regarding wake resolution, Figure 5 shows visualisation of the rotor’s wake in hover obtained using the λ_2 criterion [10].

The solver is also capable of predicting the hover performance of main rotors and results from this validation effort are given in references [3,4]. Indicative results for a hovering UH60A scale rotor [11] are given in Figure 6 where excellent agreement can be seen between the CFD results and the tunnel measurements for the chord-wise C_p distribution at various radial stations along the blade, having made allowance for elastic deflections as described by Dindar [12].

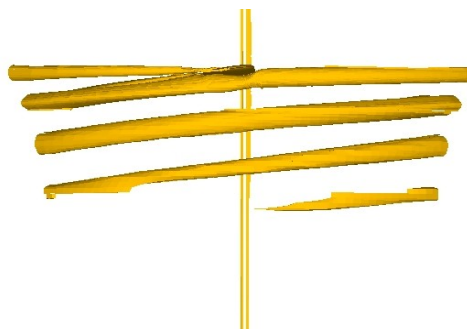


Figure 5. Wake visualisation for the hovering TRB-000 tail rotor, 10 degrees of collective, zero coning. The λ_2 criterion has been used to highlight the location of the vortex core and the obtained wake contraction.

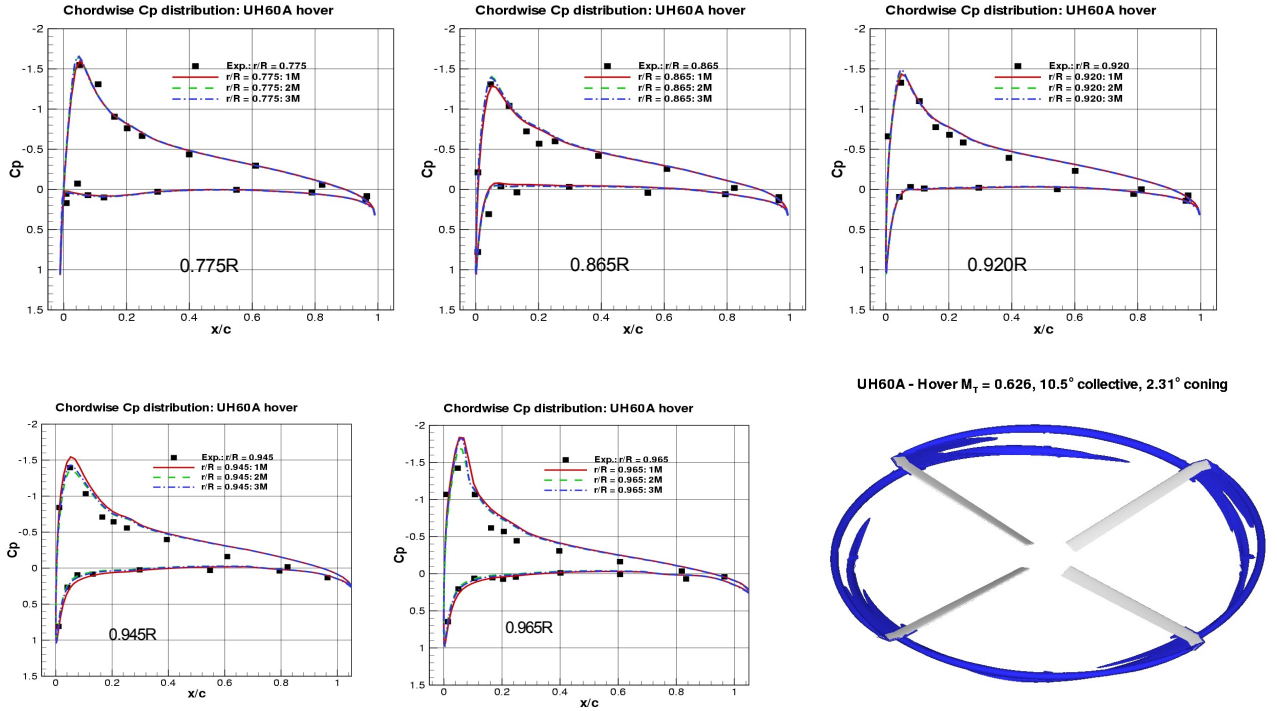


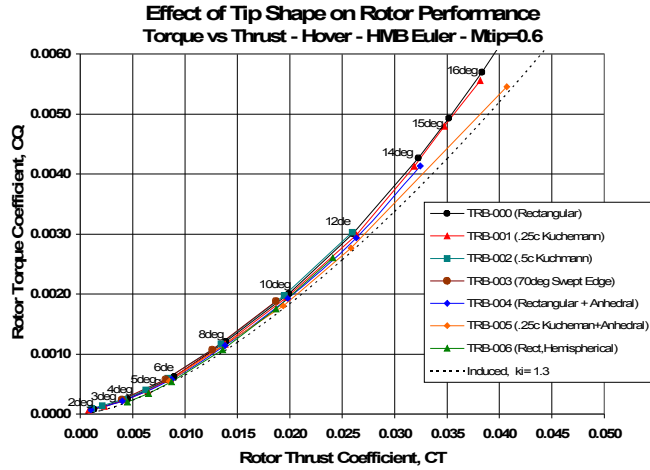
Figure 6. Prediction for the C_p distribution for the hovering UH60A model rotor of [11].

5. TAIL ROTOR CFD - RESULTS AND DISCUSSION

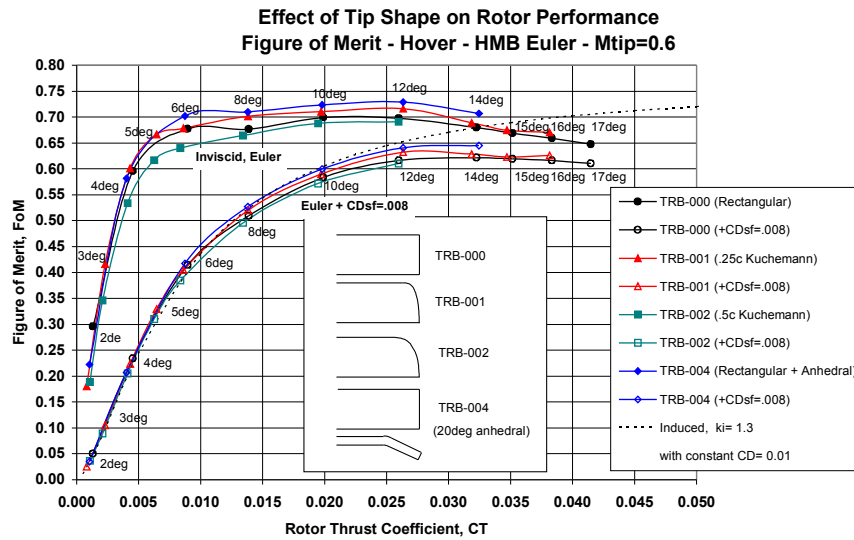
5.1 Inviscid CFD Results

In keeping with the model rotor tests, the CFD simulations reveal results for the overall performance of the rotor and the induced and profile power contributions are combined. The CFD results were therefore analysed using techniques developed for parameterising the model rotor data. For the Euler solutions, the power losses are small, and the main interest was to identify differences in induced power. The induced power factor, k_i , was determined by plotting C_Q versus $C_T^{1.5}$ and using a second order curve fit to consistently determine a value of the slope. The coefficient of the second order term in all cases was found to be relatively small and, while it is difficult to separate induced and profile power (for the Euler results this is only arises from numerical effects, and is at most only 1/10 of the normal value), the results were confirmed by plotting the residual 'profile-power' against blade loading. It was found that there was very little variation of induced power with thrust, despite the likelihood for non-linear wake effects.

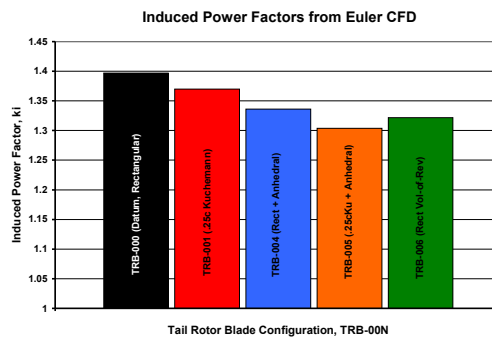
The CFD results for various tip designs are compared for untwisted blades with the same NACA0012 aerofoil, at a typical full-scale Mach number of 0.6. All CFD grids have been refined to allow a similar resolution of the wake for which vortices can be seen for 1 complete revolution (4 blade passes). Figure 7 shows a comparison of Euler results in terms of rotor torque (Fig 7a) and FoM (Fig 7b) and induced power factor, k_i , for several tail rotor designs in hover, and reveals benefits due to tip shape and anhedral.



(a)



(b)



(c)

Figure 7. Comparison of four tail rotor designs in terms of figure of merit.

The induced power factor for the datum blade was found to agree well with experiment (fig 7c), and gives confidence in the method. Note that the ki for a tail rotor is normally significantly greater than that for a main rotor and this trend has also been seen in similar computational studies for main

rotors. Ahead of the Navier-Stokes results, a constant, arbitrary amount of profile power may be added to give realistic FoM values. In particular, the results show clear benefits of using a well designed tip shape and anhedral. This set of results allows insight to be developed for the performance of each tip shape. Clearly, the datum blade represents the worst case (for the results illustrated here) though differences between the designs are subtle and CFD is perhaps the only method capable of demonstrating and separating these. The relative performance of the various tip shapes with respect to the induced power coefficient is given in Figure 7c. TRB-005 appears to perform very well in comparison with the datum TRB000 design. TRB-004 and 006 also show substantial improvement. The observed changes in the performance due to the various tip configurations can be explained by comparing the vortex wake trajectories, as shown in Figure 8 and the blade-loading distributions (Figure 9).

The comparison of the loading and moment distribution of the TRB-005 (tip with anhedral) and TRB-001, the same tip but without anhedral, is of significant importance. As can be seen in Figure 9, the anhedral reduces the tip loading and slightly increases the loading inboard. Starting from this observation and the general view that increasing rotor twist has similar effects, a study was conducted where the datum blade performance was assessed for three levels of linear twist (0, 8 and 16 degrees). The results from this study are compared in Figure 10a against model rotor test data. A first observation is that the HMB solver produced results in good agreement with the test, up until the point where the Euler solution cannot be trusted due to the increased influence of viscous effects. This set of results were plotted (Fig. 10b) vs $C_T^{3/2}$ and a polynomial of second order was fitted to the thrust data to reveal induced power factors as low as 1.2. Of course, this set of results lacks the viscous contributions to power and consequently falls below the experimental data. On the other hand, the predictions show the correct trends for induced power and results are as expected for inviscid flow simulations.

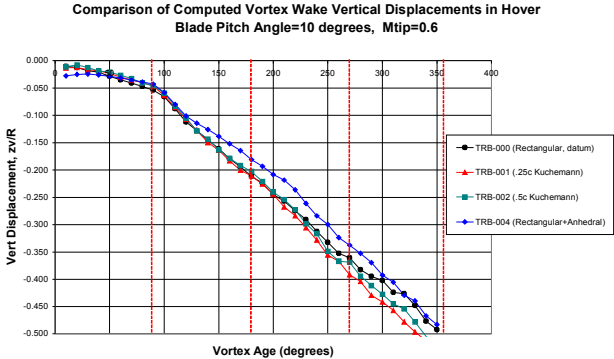


Figure 8. Comparison of four tail rotor designs in terms of vertical vortex displacement.

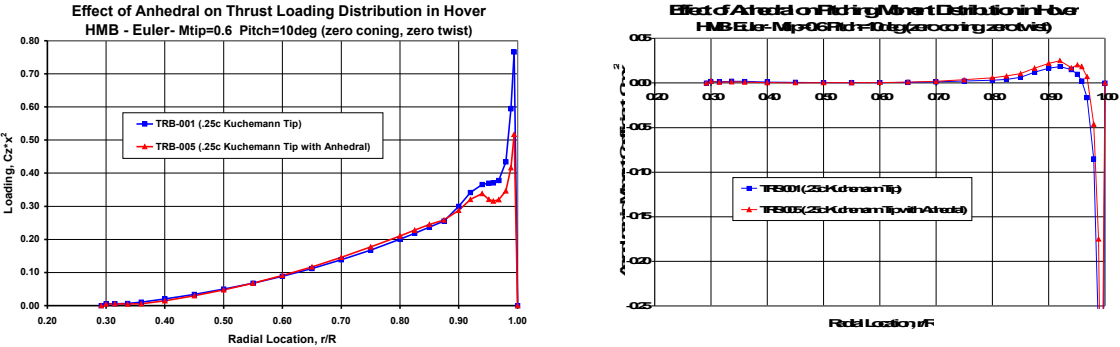


Figure 9. Assessment of the effect of tip anhedral on the span-wise loading of a tail rotor.

Most interesting is the spanwise loading shown in Figure 10c. The effect of twist is clearly demonstrated and the results show the increase in inboard loading with a corresponding reduction in the tip region. The reduction in the moment coefficient obtained by using increased twist is shown in Figure 10d. On the same Figure, results from a hover prediction method driven by test data are also plotted. Not surprisingly, most of the differences between the two methods are concentrated in the non-linear tip region. Clearly, CFD is a far more reliable tool for the analysis of the rotor performance when advanced tip configurations are used. The comparison between the effects of anhedral and twist generate quite useful insights in terms of the design of tail rotors, suggesting that a design engineer can select between twist and anhedral as a mechanism for reducing tip loading or even opt for a combination of the two contributions. This is a good example of how CFD can be used to generate useful understanding for design purposes.

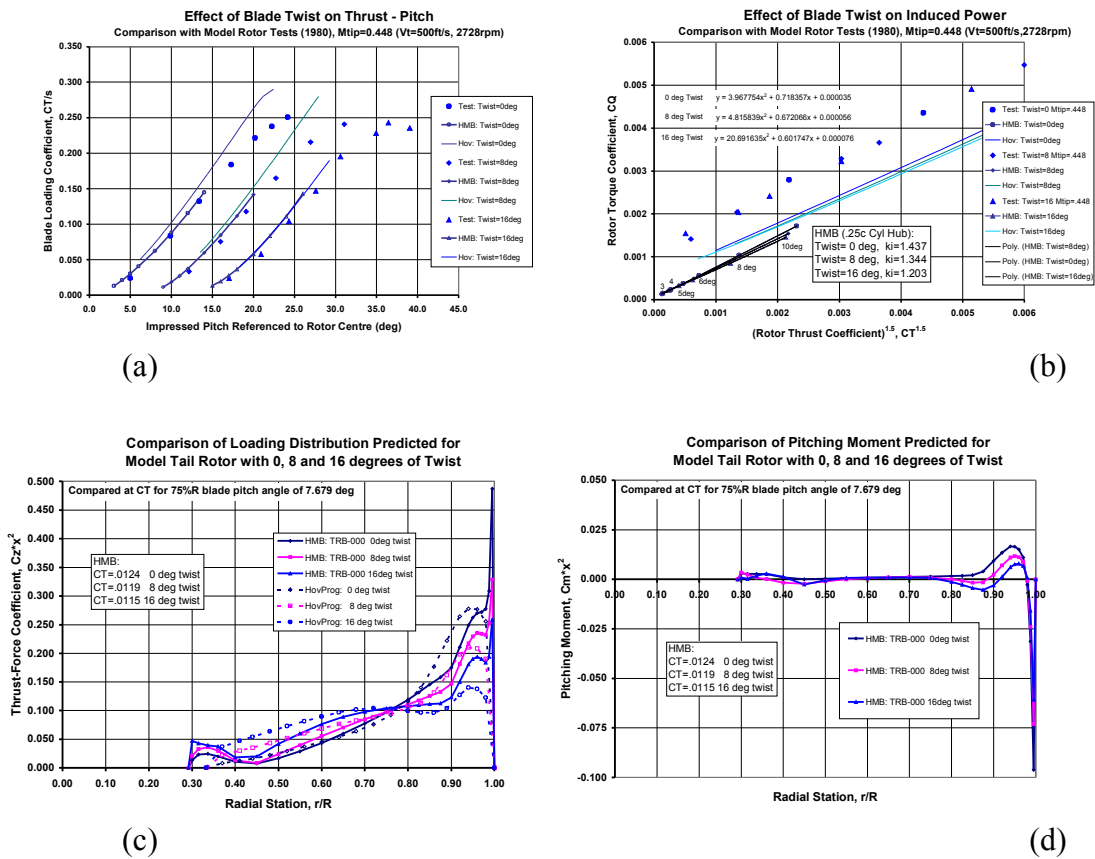


Figure 10. Assessment of the effect of twist. (a) comparison against test data, (b) reduced data for k_i computation, (c) span-wise loading and (d) span-wise moment distributions.

5.2 Viscous CFD Results

In this part of the work, the Navier-Stokes equations have been used to extend the simulations to include viscous effects which are dominant at high pitch angles near stall while the Euler model was used for screening the various designs in order to identify cases to be computed using the computationally more expensive Navier-Stokes flow model.

The quantification of viscous effects was the first objective set for this phase of the work which started from the TRB-005 design, due to its good performance characteristics in terms of induced power factor (Figure 7c).

Figure 11a presents a comparison between viscous and inviscid solutions for vertical displacement of the tip vortex. The viscous results have the same trend as the inviscid ones and the two sets of data agree well very close to the tip. Further away, the NS solution indicates a slightly larger wake radius. Small differences in the vertical displacement as a function of age are seen in Figure 11b. In terms of the velocity along the vortex trajectory, deduced from the slope of the line in Figure 11c, the two solutions agree quite well which indicates that for this rotor, Euler solutions can perhaps be used for preliminary comparison of designs for collective settings of up to about 10 degrees. A comparison of the viscous results with inviscid solutions for various tip shapes, and TRB-005 in particular, is plotted in Figure 11d. Note that for both Euler and Navier-Stokes results the vortex position at the first blade passage is higher for the anhedral tip than for the datum blade.

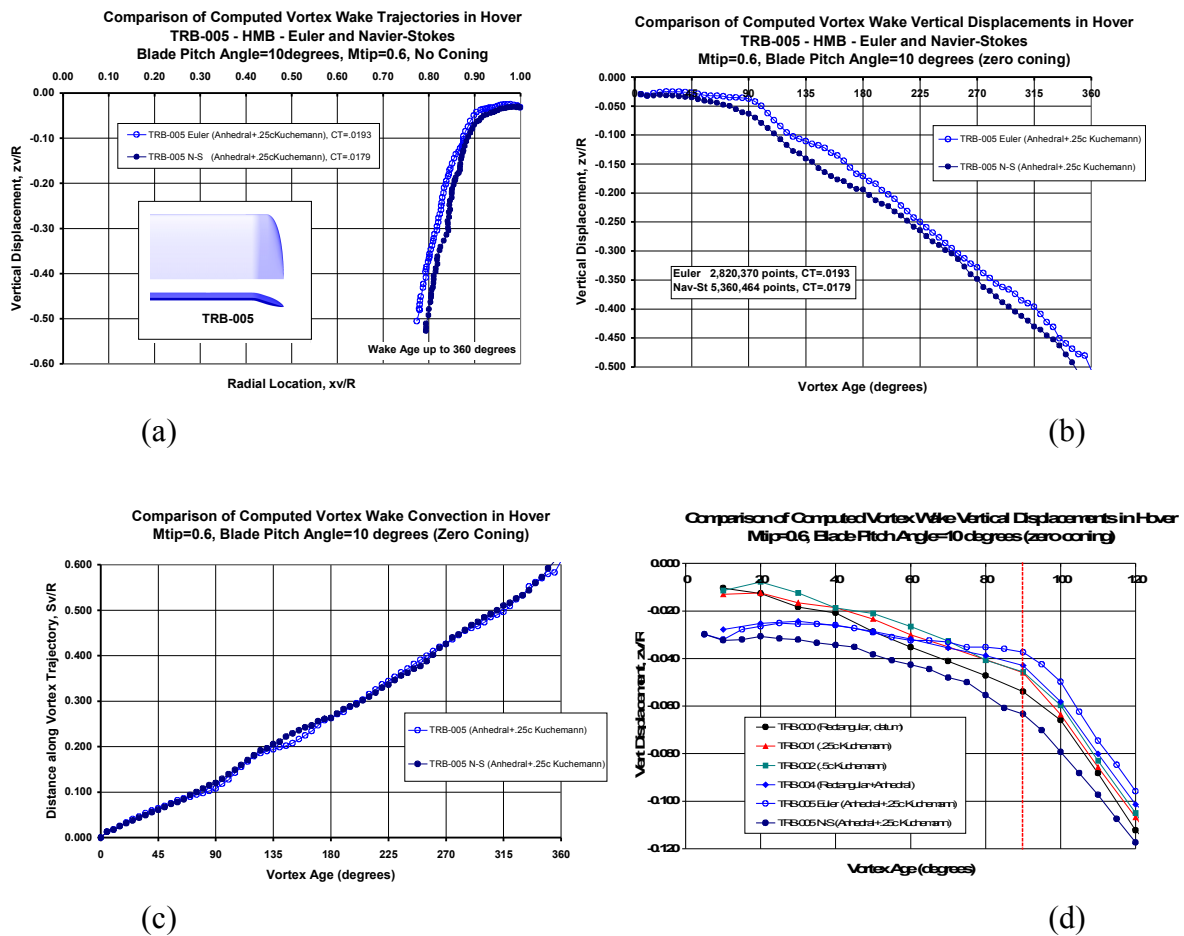


Figure 11. Comparison between Euler and Navier-Stokes results for the TRB005 rotor.

6. SUMMARY AND FUTURE STEPS

In this paper, CFD was used as a tool for predicting the hover performance of several rotor blade designs at low to moderate thrust levels. The method has been validated against published experimental data and further comparisons have been presented here against model tail rotor tests.

The thrust-pitch characteristics and the induced power factor deduced from the computations were found to agree well with experiment, and vortex locations in the wake are also well predicted.

The results of the simulations have revealed subtle differences in the performance of the various rotor tip shapes considered, and the HMB method has been found to be robust and reliable across the range of conditions. The effects of tip anhedral and twist were found to be broadly similar, resulting in a better distribution of the span-wise blade loading with lower tip loads and moments in hover. Euler computations were used where possible, due to their efficiency. Comparisons against Navier-Stokes solutions have resulted in similar conclusions for the moderate thrust conditions explored to date.

At present, this work is directed towards the study of selected tail rotor blades near the stall boundary using the Navier-Stokes equations and the unsteady, time-accurate formulation of the solver. In parallel, several of the designs presented here have also been assessed in edge-wise forward flight using the same CFD technique in order to confirm the overall viability of employing tail rotor blades with anhedral. Results from these studies are to be reported in future papers.

ACKNOWLEDGEMENT

The authors wish to thank Robert Harrison, AgustaWestland (Yeovil), and Richard Markiewicz of DSTL, for permission to publish the model rotor data.

REFERENCES

- [1] J.G. Leishman, *Principles of Helicopter Aerodynamics*, J.G. Leishman, Cambridge Aerospace Series, NY, 2000.
- [2] G. Barakos, R.Steijl, K. Badcock and A. Brocklehurst, “*Development of CFD Capability for Full Helicopter Engineering Analysis*”, Proceedings of the 31st European Rotorcraft Forum, 13-15 September 2005, Florence, Italy.
- [3] R. Steijl, G. Barakos and K. Badcock, “*A Framework for CFD Analysis of Rotors in Hover and Forward Flight*”, Int. J. for Num. Meth. in Fluids, vol. 51, 2006, pp. 819-847.
- [4] S. Osher and S. Chakravarthy, “*Upwind Schemes and Boundary Conditions with Applications to Euler Equations in General Geometries*”, Journal of Computational Physics, vol 50, 1983, pp. 447-481.
- [5] A. Jameson, “*Time Dependent Calculations using Multigrid, with Applications to Unsteady Flows past Airfoils and Wings*”, AIAA Paper 91-1596, 1991.
- [6] A. Spentzos, G. Barakos, and Badcock, P. Richards, B.E. Wenert, S. Schreck, and M. Raffel, “*CFD Investigation of 2D and 3D Dynamic Stall*”, AIAA Journal, vol 34, no 5, 2005, pp. 1023–1033.
- [7] R. Morvant, K. Badcock, G. Barakos, and B.E. Richards, “*Aerofoil-Vortex Interaction Using the Compressible Vorticity Confinement Method*”, AIAA Journal, vol 43, no 1, 2004. pp. 63–75.
- [8] J.D. Kocurek and J.L. Tangler, “*A Prescribed Wake Lifting Surface Hover Performance Analysis*”, Proceedings of the 32nd Annual Forum of the American Helicopter Society. Washington, D.C. May 10-12, 1976.
- [9] J. Jeong and F. Hussain, “*On the identification of a vortex*”, J. Fluid Mechanics, vol. 285, 1995, pp. 69-94.
- [10] P.F., Lorber, ”*Aerodynamic Results of a Pressure- Instrumented Model Rotor Test at the DNW*”, Journal of the American Helicopter Society, vol 36, no 4, 1991.
- [11] M. Dindar, et al., “*Effect of Tip Vortex Resolution on the UH-60A Rotor Blade Hover Performance Calculations*”, 54th Annual Forum of the American Helicopter Society, Washnigton, D.C., May, 1998.